Current Journal of Engineering and Science Research
Volume 3, Issue 5, pp 1-9, May-2026
ISSN (online): 3049-1738
DOI: https://doi.org/10.47001/CJESR/2026.305001
Available Online at https://www.cjesr.com

Strength Analysis of Welded Joints on Railway Bogie Side Frame with Welding Current Variations Using the Finite Element Method

[1]Ojo Kurdi, [2]*Achmad Widodo, [3]Toni Prahasto, [4]Muhammad Rizky Hidayat

[1,2,3,4]Faculty of Engineering, Department of Mechanical Engineering, Diponegoro University, Indonesia
*Corresponding Author's E-mail: Awidodo2010@gmail.com

Abstract: The quality of welded joints on railway bogie side frames is a critical factor in ensuring the structural integrity and operational safety of rail vehicles. This study investigates the effect of welding current variations on the mechanical strength of butt-joint welds on SM490 steel, which is widely used in bogie frame fabrication. Welding was performed using the Gas Metal Arc Welding (GMAW) method with an ER70S-6 filler wire of 1.2 mm diameter and welding currents of 180 A, 200 A, 220 A, and 240 A on 14 mm thick plate specimens. Tensile testing was carried out in accordance with the ASTM E8/8M standard to evaluate maximum tensile strength, elongation, and elastic modulus. The results show that a welding current of 200 A produced the highest ultimate tensile strength of 368 MPa and the greatest elongation of 33%, indicating optimal fusion and penetration at this current level. Numerical analysis using the Finite Element Method (FEM) through ANSYS Workbench was subsequently performed on the side frame geometry under three loading conditions based on EN 13749: static vertical load, longitudinal load (acceleration and braking), and lateral load (cornering). The maximum von Mises stress of 165.53 MPa occurred under the cornering condition, with a minimum safety factor of 1.69, both of which remain within acceptable structural limits. Validation of FEM results against experimental data demonstrated consistent trends in mechanical performance across all current variations, confirming the reliability of the numerical approach. These findings establish 200 A as the optimal welding current for SM490 butt-joint welds on railway bogie side frames and provide a validated numerical reference for structural design in rail vehicle manufacturing.

Keywords: SM490 Steel, Bogie Side Frame, GMAW Welding, Welding Current Variation, Tensile Strength, Finite Element Method, ANSYS; EN 13749.

I. INTRODUCTION

Transportation is a fundamental element of modern civilization, encompassing the movement of people and goods from one location to another in an efficient and safe manner. Among the various modes of transportation available, railway systems offer distinct advantages, including low emissions, high passenger and freight capacity, dedicated infrastructure, and favorable safety records over both short and long distances [1]. As urbanization accelerates globally, the demand for reliable and efficient rail transportation continues to grow, driving the need for continuous innovation in the design, materials, and manufacturing processes of railway components [2].

A critical structural element within the railway vehicle system is the bogie, which serves as the primary interface between the car body and the rail. The bogie houses the wheelsets, suspension systems, braking mechanisms, and axle bearings, all of which must function cohesively to ensure stability, comfort, and safety during operation [3]. Within the bogie assembly, the side frame plays a particularly important role, as it receives and distributes loads from the secondary suspension through the bolster and transfers them to the primary suspension and wheelsets. The side frame must therefore withstand complex, multi-directional loading conditions, including vertical loads from the vehicle weight, longitudinal forces arising from traction and braking, and lateral forces induced during cornering [4].

Given its structural criticality, the integrity of the side frame is heavily dependent on the quality of its welded joints. Welding is the predominant joining method used in bogie frame fabrication, enabling the permanent assembly of structural components with high strength and dimensional accuracy.

Current Journal of Engineering and Science Research
Volume 3, Issue 5, pp 1-9, May-2026
ISSN (online): 3049-1738
DOI: https://doi.org/10.47001/CJESR/2026.305001
Available Online at https://www.cjesr.com

However, the mechanical properties of a welded joint are strongly influenced by the welding process parameters, most notably the welding current, which governs heat input, penetration depth, fusion quality, and the microstructural characteristics of the heat-affected zone (HAZ) [5]. Insufficient current leads to incomplete fusion and poor penetration, while excessive current causes overheating, grain coarsening, and potential distortion of the base material, both of which compromise joint strength [6].

The material selected for this study is SM490 structural steel, a low-alloy high-strength steel conforming to JIS G 3106 with a minimum tensile strength of 490 MPa. This material is widely employed in heavy structural fabrication, including railway bogie frames, due to its favorable combination of weldability, mechanical strength, and toughness under dynamic and impact loading [7]. Welding was performed using the Gas Metal Arc Welding (GMAW) method with an ER70S-6 filler wire, a combination commonly used for structural steel applications requiring consistent weld quality and mechanical performance [8].

To evaluate the effect of welding current variation on joint strength, tensile testing was conducted in accordance with the ASTM E8/8M standard, providing quantitative data on ultimate tensile strength (UTS), elongation, and elastic modulus for each current condition. Complementing the experimental approach, numerical simulation using the Finite Element Method (FEM) was employed to analyze the stress distribution and deformation behavior of the side frame geometry under operational loading scenarios defined by the EN 13749 standard [9]. FEM has been widely established as an effective predictive tool in structural analysis, enabling engineers to evaluate stress concentrations, deformation patterns, and safety margins with high accuracy prior to physical prototyping [10].

Previous studies have investigated related aspects of this problem. Matin et al. [11] examined the effect of welding current variation in Shielded Metal Arc Welding (SMAW) on the tensile strength, bending strength, and microstructure of API 5L X52 pipeline steel, demonstrating that intermediate current levels yielded superior mechanical properties. Suheni et al. [12] analyzed the influence of current variation and joint configuration on the tensile and impact strength of SS400 steel welded using GMAW with ER70S-6 filler, confirming that both parameters significantly affect joint performance. Huang et al. [13] evaluated the effect of welding parameters on the mechanical and corrosion properties of dissimilar metal joints between stainless steel and low-carbon steel, highlighting the importance of parameter optimization in achieving both structural strength and corrosion resistance. However, a systematic investigation combining experimental tensile testing and FEM-based structural simulation specifically for SM490 welded butt joints on railway bogie side frames across multiple current levels remains limited in the existing literature.

This study addresses that gap by presenting an integrated experimental and numerical analysis of SM490 butt-joint welds produced at welding currents of 180 A, 200 A, 220 A, and 240 A, with the aim of: (1) determining the effect of welding current on the tensile strength and ductility of the welded joints; (2) identifying the optimal welding current for structural applications on railway bogie side frames; and (3) validating the FEM simulation results against experimental data to confirm the reliability of the numerical model as a predictive design tool.

II. MATERIALS AND METHODS

2.1 Research Overview

This study employs an integrated approach combining experimental tensile testing and numerical simulation using the Finite Element Method (FEM) to investigate the effect of welding current variation on the mechanical strength of butt-joint welds on SM490 structural steel. This comprehensive engineering approach is further utilized to evaluate the structural performance of the welded side frame bogie under various critical operational loading conditions.

2.2 Base Material and Specimen Preparation

The base material used in this study is SM490A structural steel plate with a thickness of 14 mm, conforming to JIS G 3106 [7]. This material is widely used in railway bogie frame fabrication due to its adequate tensile strength, good weldability, and toughness under dynamic loading conditions. The standard mechanical properties of SM490A are summarized in Table 1.

Table 1: Standard mechanical properties of SM490A

Property	Value
Density	7800 kg/m^3
Poisson's Ratio	0.3
Modulus of Elasticity	210 GPa
Tensile Strength	490 MPa
Yield Strength	325 MPa
Elongation	22%

Tensile test specimens were prepared in accordance with

Current Journal of Engineering and Science Research
Volume 3, Issue 5, pp 1-9, May-2026
ISSN (online): 3049-1738
DOI: https://doi.org/10.47001/CJESR/2026.305001
Available Online at https://www.cjesr.com

ASTM E8/8M [9], with specimen geometry following the standard sub-size flat specimen dimensions as illustrated in Fig. 2. Prior to welding, the plate surfaces were cleaned to remove mill scale, rust, and contaminants that could adversely affect weld quality.

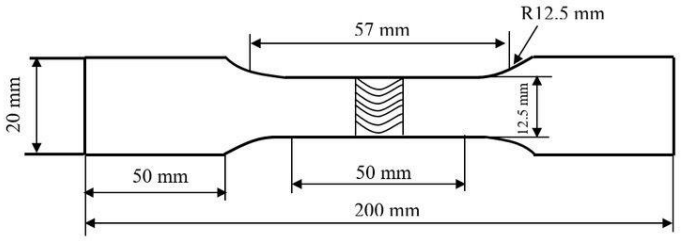

Figure 1: Specimen Geometry ASTM E8

2.3 Welding Process and Current Variation

Welding was performed using the Gas Metal Arc Welding (GMAW) method, employing an ER70S-6 solid wire electrode with a diameter of 1.2 mm. The joint configuration used was a butt joint, which represents the primary joint type found in side frame bogie construction. The welding voltage was maintained constant at 25 V throughout all specimens, while the welding current was systematically varied at four levels: 180 A, 200 A, 220 A, and 240 A, as detailed in Table 2.

Table 2: Welding parameters for each current variation

No.	Variable	Fixed Parameters	Welding Current (A)
1	Material	SM490 (14 mm thick)	–
2	Joint Type	Butt Joint	–
3	Filler Wire	ER70S-6 (Ø 1.2 mm)	–
4	Welding Current	–	180, 200, 220, 240
5	Voltage	25 V	–

Each current variation was applied to produce welded plate specimens of equal weld length, ensuring consistency in the comparison of mechanical properties across all test conditions. The welding quality standard adopted in this study follows ASME Section IX, which specifies the qualification requirements for welding procedure specifications (WPS) and welder performance qualifications (WPQ) through mechanical testing [14].

2.4 Tensile Testing

Tensile testing was conducted using a Universal Testing Machine (UTM) following the ASTM E8/8M standard procedure. Prior to testing, the initial gauge length (L_0) and cross-sectional diameter (d_0) of each specimen were measured and recorded. The specimens were securely clamped in the upper and lower gripping heads of the UTM, and axial tensile loading was applied at a controlled rate until fracture. The following mechanical properties were recorded and calculated from each test:

- Ultimate Tensile Strength (UTS), calculated as:

$$\sigma_u = \frac{F_m}{A_0}$$

- Elongation (%), calculated as:

$$\%EL = \frac{L_1 - L_0}{L0} \times 100\%$$

- Elastic Modulus (E), calculated as:

$$E = \frac{\Delta\sigma}{\Delta\varepsilon}$$

where F_m is the maximum load, A_0 is the original cross-sectional area, L_0 and L_1 are the initial and final gauge lengths, respectively.

Additionally, density measurements were performed using the water displacement method, and Poisson's ratio was determined from the measured changes in gauge length and diameter before and after fracture. These material properties were subsequently used as input parameters for the FEM simulation.

2.5 Finite Element Method (FEM) Simulation

2.5.1 Geometry and Software

Numerical simulation was performed using ANSYS Workbench 2024 R2 under the Static Structural module. The side frame geometry was modeled in SolidWorks and imported into ANSYS in .SLDPRT format. The model represents the actual side frame bogie geometry with key dimensions as listed in Table 3.

Table 3: Side frame bogie geometric specifications

Parameter	Value	Unit
Width of Bogie Frame	2240	mm
Bogie Wheel Base	2560	mm
Bogie Length	3534	mm
Bogie Width	*3030*	mm

Current Journal of Engineering and Science Research
Volume 3, Issue 5, pp 1-9, May-2026
ISSN (online): 3049-1738
DOI: https://doi.org/10.47001/CJESR/2026.305001
Available Online at https://www.cjesr.com

The global coordinate system was defined with the X-axis aligned to the longitudinal direction (direction of travel), Y-axis in the vertical direction, and Z-axis in the lateral direction.

2.5.2 Material Properties

Material properties assigned in the simulation were derived from the experimental tensile test results for each welding current variation. The mechanical properties of the welded material at 200 A — identified as the optimal current — are presented in Table 4, and were used as the primary input for the main simulation.

Table 4: Mechanical properties of welded SM490 at 200 A

Property	Value
Density	7530 kg/m³
Young's Modulus	190 GPa
Yield Strength	280.1 MPa
Ultimate Tensile Strength	368.0 MPa
Elongation	33%
Poisson's Ratio	0.31

2.5.3 Meshing

The geometry was discretized using three-dimensional tetrahedral solid elements. A mesh convergence study (grid independence test) was conducted by systematically varying the element size from 12.8 mm to 12.4 mm and observing the change in maximum von Mises stress. The results of the convergence study are presented in Table 5.

Table 5: Grid independence test results

No.	Element Size (mm)	Number of Elements	Max. Stress (MPa)	Error (%)
1	12.8	191,491	366.01	–
2	12.7	192,073	368.03	0.50
3	12.6	194,285	364.07	0.31
4	12.5	253,857	364.24	0.25
5	12.4	213,711	364.40	0.17

An element size of 12.5 mm was selected as the optimal mesh size, as the change in maximum stress between successive refinements fell below the 1% convergence threshold, ensuring grid-independent results while maintaining computational efficiency. Mesh refinement was applied at the weld joint region, which represents the critical zone of maximum stress concentration during operation.

2.5.4 Boundary Conditions and Loading

Three load cases were defined based on EN 13749, representing the principal operational loading scenarios experienced by the bogie side frame [9]. The applied forces and boundary conditions for each scenario are summarized in Table 6.

Table 6: Summary of load cases based on EN 13749

Load Case	Vertical [N]	Longitudinal Shunt/Dec./Yaw [N]	Longitudinal Gearbox [N]	Braking [N]	Transversal [N] Bump Stop	Transversal [N] Air Spring
1	128070	*	*	*	*	*
2	128070	*	*	*	89.678	4.401
3	128070	176.580	*	*	*	*

Forces were applied using the Remote Force feature in ANSYS Workbench at the bearing pad contact surfaces between the bogie structure and the car body. The output parameters evaluated from each simulation were maximum von Mises stress, total deformation, and safety factor against yield strength.

III. RESULTS AND DISCUSSIONS

3.1 Tensile Test Results

3.1.1 Effect of Welding Current on Mechanical Properties

The tensile test results for SM490 butt-joint specimens welded at four current levels are presented in Table 7. Each value represents the average of two specimens tested under identical conditions.

Table 7: Tensile test results for each welding current variation

Welding Current (A)	Force Peak (kN)	UTS (MPa)	Elongation (%)
180	61.9	353	32.0
200	64.4	368	33.0
220	62.5	357	28.0
240	63.1	360	31.0

The results demonstrate that welding current has a significant influence on the mechanical properties of the welded joint. The highest UTS of 368 MPa and the greatest elongation of 33% were both achieved at a welding current of 200 A, indicating that this current level produces the most favorable combination of heat input, fusion depth, and microstructural quality. At 180 A, the UTS of 353 MPa is comparatively lower, likely attributable to insufficient heat input resulting in incomplete fusion and shallow penetration at the weld interface. At 220 A and 240 A, although the force peak values show a slight recovery compared to 180 A, the UTS values of 357 MPa

Current Journal of Engineering and Science Research
Volume 3, Issue 5, pp 1-9, May-2026
ISSN (online): 3049-1738
DOI: https://doi.org/10.47001/CJESR/2026.305001
Available Online at https://www.cjesr.com

and 360 MPa respectively remain below the peak achieved at 200 A. This decline in performance at higher currents is consistent with the formation of a coarser microstructure and an enlarged heat-affected zone (HAZ) caused by excessive heat input, both of which are known to reduce joint strength and ductility [6]. Furthermore, the sharp drop in elongation to 28% at 220 A, followed by a partial recovery to 31% at 240 A, suggests that the thermal cycle at 220 A promotes the formation of harder, more brittle microstructural phases within the HAZ, which are partially mitigated at 240 A due to differences in the post-weld cooling rate.

It is noted that all specimen UTS values fall below the standard minimum tensile strength of 490 MPa specified for SM490 base material under JIS G 3106. This is an expected outcome in welded joints, as the thermal cycle inherently alters the microstructure of the weld metal and HAZ relative to the unaffected base material. Nevertheless, all specimens exhibit elongation values exceeding 22% and yield strength values consistent with structural adequacy, confirming their suitability for use as input parameters in the FEM simulation [7].

3.1.2 Fracture Mode and Specimen Condition

Visual examination of the fractured specimens revealed ductile fracture behavior across all current variations, characterized by necking at the weld region prior to final separation. This observation is consistent with the inherent ductility of SM490 low-carbon structural steel. At 200 A, the fracture surface showed the most uniform distribution, reflecting well-distributed stress across the weld cross-section and confirming optimal fusion quality. At 240 A, a slightly wider melting zone was observed on the specimen surface, indicative of the greater heat input at this current level, though no significant macro-defects such as porosity or undercutting were detected.

3.2 FEM Simulation Results

3.2.1 Static Load Case

Under static vertical loading, the maximum von Mises stress was 56.973 MPa with a total deformation of 0.0735 mm, and a safety factor well above 2.0. The contour plots of von Mises stress, total deformation, and safety factor for the static load case are presented in Figs. 3(a), 3(b), and 3(c), respectively.

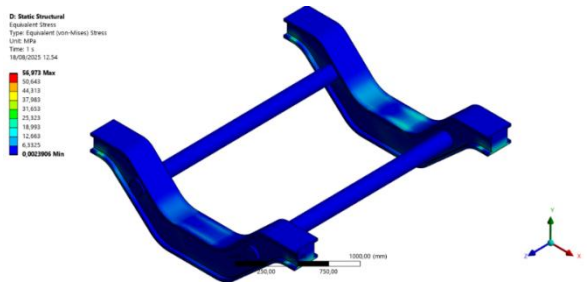

Figure 2(a): Von Mises stress distribution

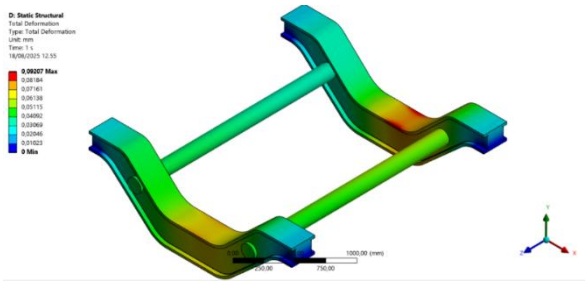

Figure 2(b): Total deformation distribution

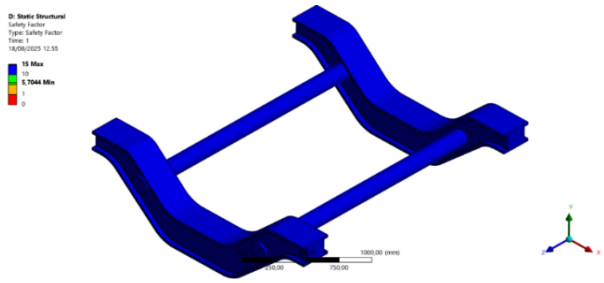

Figure 2(c): Safety factor

The stress distribution was well-dispersed across the side frame structure, with the highest stress concentration observed at the junction between the side frame and the bolster seat, as shown in Fig. 3(a). The low deformation value shown in Fig. 3(b) confirms the high structural stiffness of the side frame geometry under gravitational loading alone. The safety factor contour in Fig. 3(c) indicates that the entire structure maintains a substantial margin against yielding, with the minimum safety factor remaining well above 2.0 under this loading condition.

3.2.2 Longitudinal Load Case (Acceleration and Braking)

Under the combined vertical and longitudinal loading condition, the maximum von Mises stress increased to 72.875 MPa with a total deformation of 0.0921 mm and a safety factor of 5.70. The contour plots are presented in Figs. 4(a), 4(b), and 4(c).

Current Journal of Engineering and Science Research
Volume 3, Issue 5, pp 1-9, May-2026
ISSN (online): 3049-1738
DOI: https://doi.org/10.47001/CJESR/2026.305001
Available Online at https://www.cjesr.com

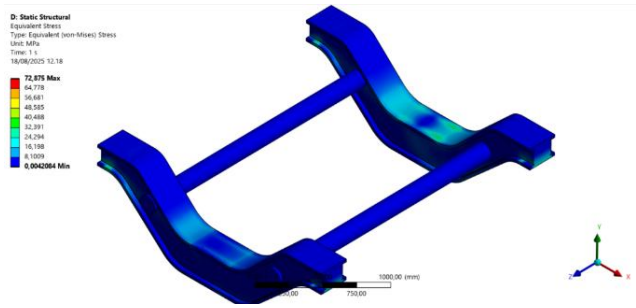

Figure 3(a): Von Mises stress distribution

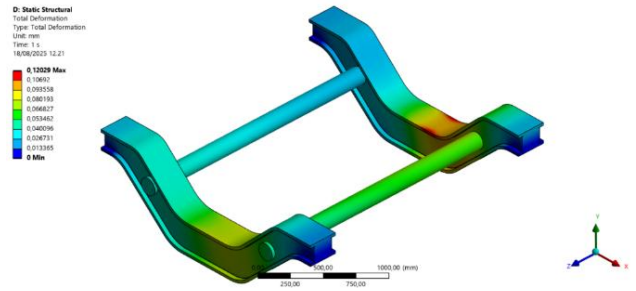

Figure 3(b): Total deformation distribution

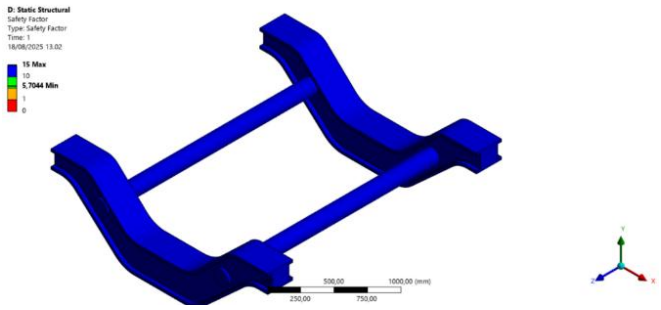

Figure 3(c): Safety factor

As shown in Fig. 4(a), the stress distribution remained uniform without significant stress concentration hotspots at the weld joint area. The maximum deformation of 0.0921 mm shown in Fig. 4(b) was identified at the connection between the side frame and the cross beam, which represents the critical zone under longitudinal inertial loading. The safety factor distribution in Fig. 4(c) confirms that the welded joint at 200 A maintains a high structural safety margin of 5.70, demonstrating reliable resistance against plastic deformation under dynamic longitudinal loading.

3.2.3 Lateral Load Case (Cornering)

The cornering condition produced the most critical structural response among all load cases. The contour plots of von Mises stress, total deformation, and safety factor are presented in Figs. 5(a), 5(b), and 5(c).

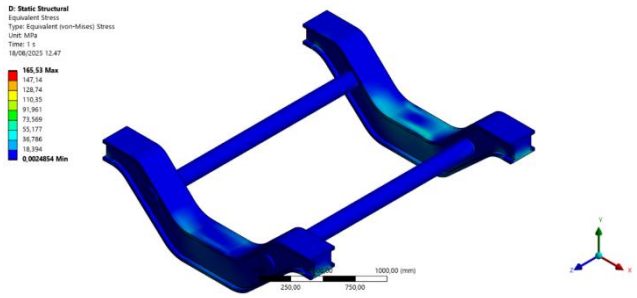

Figure 4(a): Von Mises stress distribution

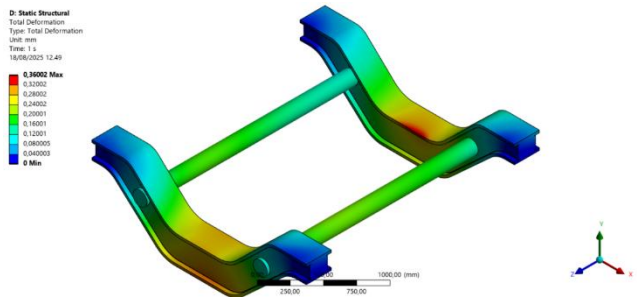

Figure 4(b): Total deformation distribution

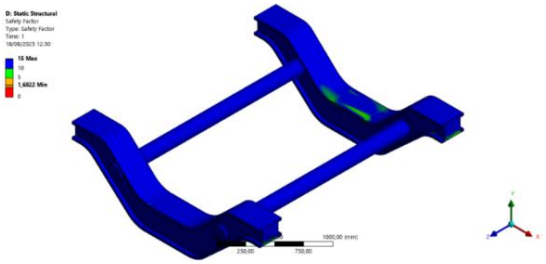

Figure 4(c): Safety factor

As shown in Fig. 5(a), the maximum von Mises stress of 165.53 MPa occurred at the weld joint area and axle seat region, indicated by the red zone in the contour plot. The elevated stress in this condition is attributed to the combined effect of centrifugal lateral force and the resulting twisting moment acting on the side frame during curve negotiation. The deformation contour in Fig. 5(b) shows a maximum total deformation of 0.3600 mm, distributed primarily along the outer side of the structure, reflecting the combined bending and torsional response under lateral loading. The safety factor contour in Fig. 5(c) shows a minimum value of 1.69, which represents the lowest margin across all load cases. Although still above the minimum acceptable threshold of 1.0, this value highlights the cornering

Current Journal of Engineering and Science Research
Volume 3, Issue 5, pp 1-9, May-2026
ISSN (online): 3049-1738
DOI: https://doi.org/10.47001/CJESR/2026.305001
Available Online at https://www.cjesr.com

condition as the governing design scenario for the welded side frame, particularly with respect to long-term fatigue performance of the weld joint.

3.3 Comparison of Simulation Results Across Current Variations

To further evaluate the influence of welding current on structural performance, comparative bar charts of von Mises stress, total deformation, and safety factor across all current variations (180 A, 200 A, and 220 A) are presented in Figs. 6–8 for each load case.

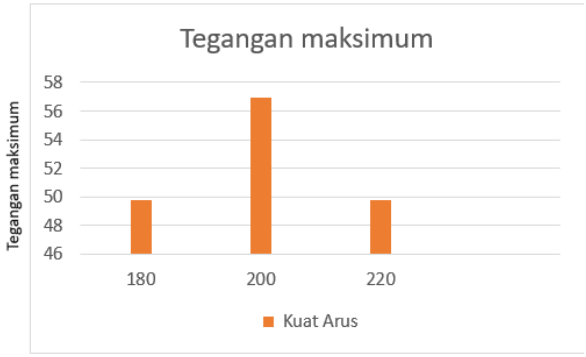

Figure 5(a): Comparison of von Mises stress for static load

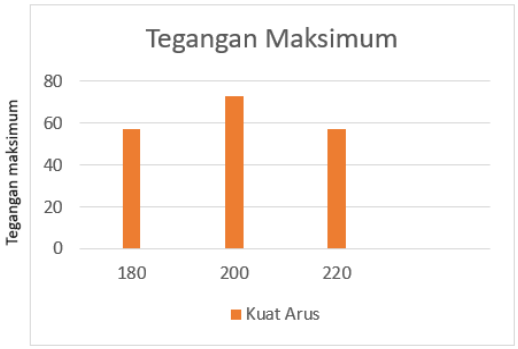

Figure 5(b): Comparison of von Mises stress for longitudinal load

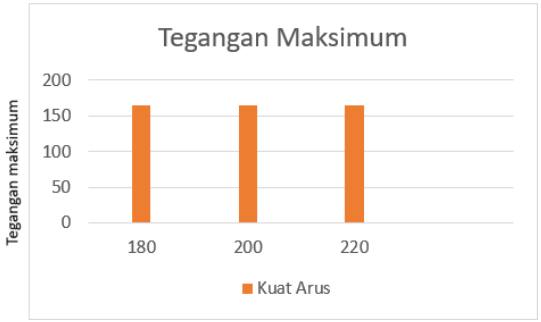

Figure 5(c): Comparison of von Mises stress for cornering load

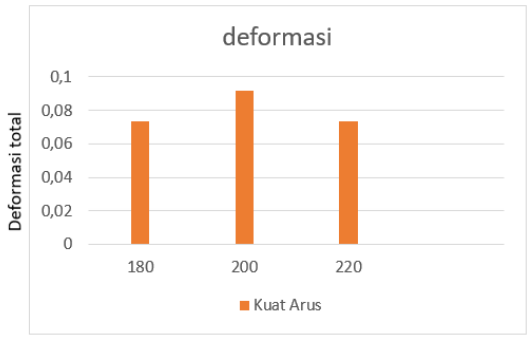

Figure 6(a): Comparison of total deformation for static load

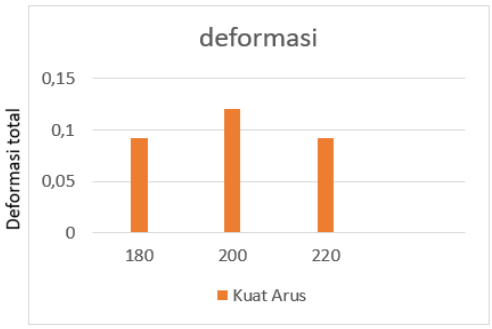

Figure 6(b): Comparison of total deformation for longitudinal load

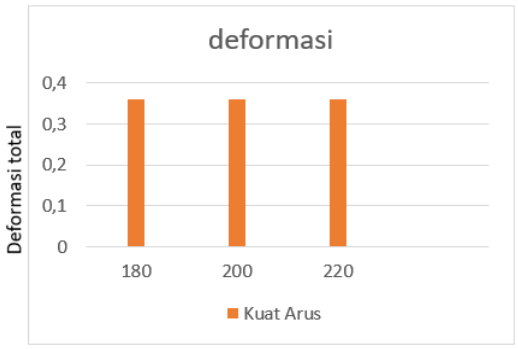

Figure 6(c): Comparison of total deformation for cornering load

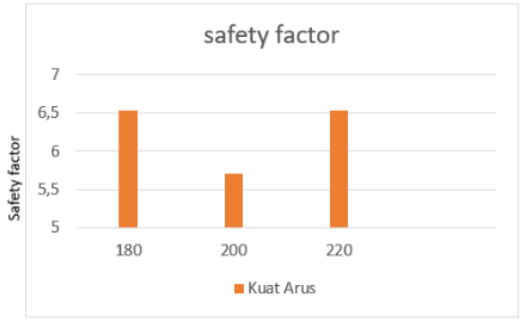

Figure 7(a): Comparison of safety factor for static load

Current Journal of Engineering and Science Research
Volume 3, Issue 5, pp 1-9, May-2026
ISSN (online): 3049-1738
DOI: https://doi.org/10.47001/CJESR/2026.305001
Available Online at https://www.cjesr.com

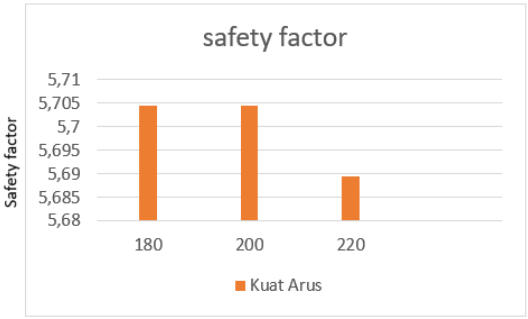

Figure 7(b): Comparison of safety factor for longitudinal load

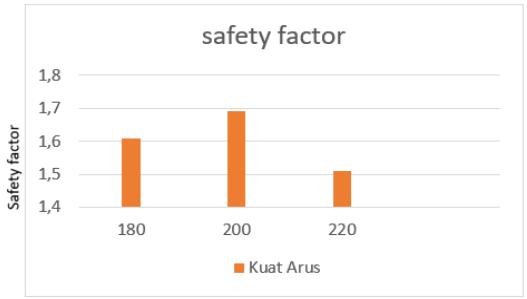

Figure 7(c): Comparison of safety factor for cornering load

The comparative analysis consistently shows that the 200 A welded specimen produces the most favorable structural response across all three loading conditions, exhibiting the lowest maximum von Mises stress and total deformation, alongside the highest safety factor. This result is in strong agreement with the experimental tensile test findings, where 200 A also yielded the highest UTS and elongation values. The 180 A specimens exhibited higher stress concentrations and lower safety factors compared to 200 A, attributable to the weaker joint properties resulting from incomplete fusion. The 220 A specimens showed intermediate structural performance, reflecting partial degradation of joint properties due to excessive heat input and HAZ coarsening. These trends are consistent with findings reported by Matin et al. [11] and Suheni et al. [12], who similarly observed that intermediate welding current levels yield superior mechanical performance in structural steel weldments.

IV. CONCLUSION

This study presents an integrated experimental and numerical investigation into the effect of welding current variation on the mechanical strength of SM490 butt-joint welds and the structural performance of a railway bogie side frame. Based on the tensile test results and FEM simulation analysis conducted across three representative operational load cases in accordance with EN 13749, the following conclusions are drawn:

1. Welding current significantly influences the mechanical properties of SM490 butt-joint welds produced by the GMAW process. Among the four current levels investigated — 180 A, 200 A, 220 A, and 240 A — the welding current of 200 A yielded the highest ultimate tensile strength of 368 MPa and the greatest elongation of 33%, indicating optimal heat input, fusion depth, and microstructural quality at this current level.
2. Insufficient welding current (180 A) results in incomplete fusion and reduced joint strength, as evidenced by the lowest UTS of 353 MPa among all tested specimens. Conversely, excessive welding current (220 A and 240 A) promotes grain coarsening and HAZ enlargement due to elevated heat input, leading to partial deterioration of tensile strength and a notable reduction in ductility, particularly at 220 A where elongation dropped to 28%.
3. The FEM simulation confirms that all three load cases — static vertical, longitudinal (acceleration and braking), and lateral (cornering) — produce von Mises stresses well below the yield strength of the welded material, with maximum stress values of 56.97 MPa, 72.88 MPa, and 165.53 MPa, respectively. All simulated conditions satisfy the minimum safety factor requirement, confirming the structural integrity of the welded side frame under operational loading.
4. The cornering (lateral) load case governs the structural design of the welded side frame, producing the highest von Mises stress of 165.53 MPa, the largest total deformation of 0.3600 mm, and the lowest safety factor of 1.69 among all load cases. This condition should be treated as the critical design scenario, particularly in the context of long-term fatigue assessment of the weld joint.
5. The comparative FEM analysis across current variations consistently identifies 200 A as the optimal welding current, yielding the most favorable structural response — including the lowest stress concentration and the highest safety factor under the cornering condition — across all three load cases. This result is in full agreement with the experimental tensile test findings, validating the reliability and consistency of the integrated experimental–numerical approach adopted in this study.
6. The validated FEM model provides a reliable predictive framework for the structural assessment of SM490 welded joints on railway bogie side frames, and may serve as a reference for welding procedure qualification and structural design optimization in railway vehicle manufacturing in

Current Journal of Engineering and Science Research
Volume 3, Issue 5, pp 1-9, May-2026
ISSN (online): 3049-1738
DOI: https://doi.org/10.47001/CJESR/2026.305001
Available Online at https://www.cjesr.com

accordance with EN 13749 and ASME Section IX standards.

REFERENCES

[1] B. Sitorus, et al., "Railway transportation efficiency and safety: A comprehensive review," *Journal of Transportation Engineering*, vol. 12, no. 3, pp. 45–58, 2024.

[2] K. Al Amin, S. Y. Firiambodo, E. P. Purwanti, and E. W. R. Widodo, "Pengelasan pada stainless steel dengan tipe yang berbeda menggunakan resistance spot welding untuk aplikasi gerbong kereta," *Jurnal Rekayasa Mesin*, vol. 16, no. 3, pp. 1–10, 2021.

[3] S. M. Redi, A. Susanto, B. Asngali, and M. Martin, "Simulasi dinamis pada kereta penumpang stainless steel new generation menggunakan metode multibody dynamic system," *Jurnal Perkeretaapian Indonesia*, vol. 6, no. 2, pp. 49–56, 2022.

[4] R. Kurniadi, "Optimasi desain bogie frame light rail transit (LRT) dengan penambahan backing plate menggunakan finite element method," *Undergraduate Thesis, Institut Teknologi Indonesia, Tangerang, Indonesia*, 2024.

[5] M. M. Sheykhi and M. A. Mostafaei, "Optimizing weld strength and microstructure in CP-titanium and 304 stainless steel friction welds with chromium interlayer," *Results in Materials*, vol. 24, p. 100627, 2024, doi: 10.1016/j.rinma.2024.100627.

[6] Z. Zulfadly and M. A. Ghony, "Variasi ampere terhadap kekuatan tarik pada hasil pengelasan dengan posisi down hand," Hexatech: *Jurnal Ilmiah Teknik*, vol. 1, no. 1, pp. 39–50, 2022, doi: 10.55904/hexatech.v1i01.75.

[7] R. D. Sulamet-Ariobimo, J. W. Soedarsono, T. Sukarnoto, A. Rustandi, Y. Mujalis, and D. Prayitno, "Tensile properties analysis of AA1100 aluminium and SS400 steel using different JIS tensile standard specimen," *Journal of Applied Research and Technology*, vol. 14, no. 2, pp. 148–153, 2016, doi: 10.1016/j.jart.2016.03.006.

[8] N. Nishanth and K. Venkatesan, "A literature review on gas metal arc welding (GMAW)," *International Journal of Innovative Research in Technology*, vol. 370, no. 7, pp. 370–375, 2022.

[9] F. Fankhauser, J. A. Tyson, and J. Askari, "Transient structural analysis of electric bus chassis frame," *IOP Conference Series: Materials Science and Engineering*, vol. 1185, no. 1, p. 012038, 2021, doi: 10.1088/1757-899X/1185/1/012038.

[10] N. K. Pikle, S. R. Sathe, and A. Y. Vyavhare, "GPGPU-based parallel computing applied in the FEM using the conjugate gradient algorithm: a review," *Sadhana*, vol. 43, no. 7, pp. 1–21, 2018, doi: 10.1007/s12046-018-0892-0.

[11] Q. Matin, R. Haliq, A. I. Ismail, and M. Jamil, "Analysis of shielded metal arc welding (SMAW) with current variations against tensile strength, bending strength, and microstructure of API 5L X52," *Journal of Mechanical Engineering Research*, vol. 11, no. 2, pp. 1–9, 2024.

[12] Suheni, A. A. Rosidah, and S. S. Utomo, "Analisa pengaruh variasi arus dan sambungan terhadap kekuatan tarik dan impak dengan material SS400 pada pengelasan GMAW," *Jurnal Teknik Mesin Indonesia*, vol. 19, no. 1, pp. 1–8, 2024.

[13] C.-H. Huang, C.-H. Hou, T.-S. Hsieh, L. Tsai, and C.-C. Chiang, "Mechanical and corrosion properties of dissimilar welded joints between stainless steel and low-carbon steel," *Proceedings of the Institution of Mechanical Engineers, Part E: Journal of Process Mechanical Engineering*, vol. 236, no. 4, pp. 1–10, 2022.

[14] American Society of Mechanical Engineers, ASME Boiler and Pressure Vessel Code Section IX: Welding, Brazing, and Fusing Qualifications. *New York, NY, USA: ASME*, 2019.

Citation of this Article:

Ojo Kurdi, Achmad Widodo, Toni Prahasto, & Muhammad Rizky Hidayat. (2026). Strength Analysis of Welded Joints on Railway Bogie Side Frame with Welding Current Variations Using the Finite Element Method. *Current Journal of Engineering and Science Research*. 3(5), 1-9. Article DOI: https://doi.org/10.47001/CJESR/2026.305001

***** End of the Article *****